JVI Journals.ASM.org

Respiratory Syncytial Virus G Protein CX3C Motif Impairs Human Airway Epithelial and Immune Cell Responses

Tatiana Chirkova,[a] Seyhan Boyoglu-Barnum,[a] Kelsey A. Gaston,[a] Fahad M. Malik,[a] Steven P. Trau,[a] Antonius G. P. Oomens,[b] Larry J. Anderson[a]

Emory University Department of Pediatrics, Atlanta, Georgia, USA[a]; Oklahoma State University Center for Veterinary Health Sciences, Stillwater, Oklahoma, USA[b]

Respiratory syncytial virus (RSV) is a major cause of severe lower respiratory infection in infants and young children and causes disease in the elderly and persons with compromised cardiac, pulmonary, or immune systems. Despite the high morbidity rates of RSV infection, no highly effective treatment or vaccine is yet available. The RSV G protein is an important contributor to the disease process. A conserved CX3C chemokine-like motif in G likely contributes to the pathogenesis of disease. Through this motif, G protein binds to CX3CR1 present on various immune cells and affects immune responses to RSV, as has been shown in the mouse model of RSV infection. However, very little is known of the role of RSV CX3C-CX3CR1 interactions in human disease. In this study, we use an *in vitro* model of human RSV infection comprised of human peripheral blood mononuclear cells (PBMCs) separated by a permeable membrane from human airway epithelial cells (A549) infected with RSV with either an intact CX3C motif (CX3C) or a mutated motif (CX4C). We show that the CX4C virus induces higher levels of type I/III interferon (IFN) in A549 cells, increased IFN-α and tumor necrosis factor alpha (TNF-α) production by human plasmacytoid dendritic cells (pDCs) and monocytes, and increased IFN-γ production in effector/memory T cell subpopulations. Treatment of CX3C virus-infected cells with the $F(ab')_2$ form of an anti-G monoclonal antibody (MAb) that blocks binding to CX3CR1 gave results similar to those with the CX4C virus. Our data suggest that the RSV G protein CX3C motif impairs innate and adaptive human immune responses and may be important to vaccine and antiviral drug development.

Respiratory syncytial virus (RSV) is a major cause of severe bronchiolitis and pneumonia in infants and causes repeat infections throughout life (1–4). The elderly and persons with compromised cardiac, pulmonary, and immune systems are at the greatest risk of severe complications with repeat infection. Despite being a high priority for vaccine development and over 50 years of research, no RSV vaccine or highly effective treatment is available for RSV. The first vaccine, formalin-inactivated RSV (FI-RSV), led to enhanced disease upon subsequent natural RSV infection in infants and young children (5–8). Subsequently, several live attenuated RSV vaccines, a bovine parainfluenza virus vector vaccine, and protein subunit vaccines have been developed and tested in humans, but none has yet been sufficiently safe or effective to move to licensure (9). A better understanding of the pathogenesis of RSV disease will likely provide clues for successful vaccine and antiviral drug design.

The two surface glycoproteins, F and G, are responsible for inducing a protective immune response, with F inducing higher levels of neutralizing antibodies and, being more conserved, inducing better cross protection between the two major antigenic groups, A and B (10–12). The G protein induces protective immune responses but also host responses associated with disease (13); some of them are likely related to the presence of the CX3C chemokine-like motif.

The G protein is a type II glycoprotein with a cytoplasmic tail from the N terminus to amino acid (aa) 37, a membrane anchor from aa 38 to 66, a variable glycosylated domain from aa 67 to ~155, a central conserved region from aa ~155 to 206, and a variable glycosylated region from aa 207 to the C terminus (14–16). A CX3C chemokine motif is located at aa 182 to 186 in the central, relatively conserved region of G, and through this motif, G binds to CX3CR1 (17), the receptor for the host CX3C chemokine fractalkine. CX3CR1 is expressed in many cell types: neurons and microglial cells (18), monocytes (19), dendritic cells (DCs) (20), natural killer (NK) cells, and T lymphocytes (19, 21). Soluble fractalkine mediates chemoattraction of $CX3CR1^+$ immune cells to the site of inflammation, while the surface-anchored fraction of fractalkine provides cell adhesion (22). The RSV G protein competes with fractalkine for binding to CX3CR1 and mimics fractalkine's induction of leukocyte migration (17).

The RSV G protein has been associated with modulating a number of immune responses. For example, vaccination with intact G, secreted G, or some G peptides has induced Th2-biased memory responses, resulting in increased pulmonary inflammation and eosinophilia after RSV challenge (23–28). In other studies, G protein stimulation has been associated with suppression of some immune responses, such as Toll-like receptor 3 (TLR3) or TLR4 induction of beta interferon (IFN-β) (26), proinflammatory responses in lung epithelial cells (29), lymphoproliferation of T cells (30), and a number of innate responses in monocytes, macrophages, or dendritic cells (31, 32). The G protein has also been shown to enhance cytotoxic T cell responses (33, 34) and decrease expression of SOCS3 (suppressor of cytokine signaling 3) protein, which in turn downregulates type I IFN production (35). The G protein has also been associated with depression of the respiratory rate (36), increased production of pulmonary substance P (37), and suppression of antibody-mediated clearance of virus (38, 39).

Received 27 June 2013 **Accepted** 26 September 2013
Published ahead of print 2 October 2013
Address correspondence to Larry J. Anderson, larry.anderson@emory.edu.

doi:10.1128/JVI.01741-13

Some of these G-mediated effects have been associated with the G protein-CX3CR1 interaction, including impaired CD4 and CD8 T cell trafficking to the lungs and cytotoxicity of $CX3CR1^+$ cells (40), enhanced pulmonary inflammation in RSV-challenged FI-RSV-vaccinated mice (41), and G protein-induced suppression of respiratory rates in mice (36). However, little is known of the impact of the RSV G protein CX3C motif on infections in humans.

To study the role of the CX3C motif in human RSV disease, we employed an *in vitro* model comprised of both human airway epithelial cells (A549 cells) and human immune cells (peripheral blood mononuclear cells [PBMCs]). Most previous *in vitro* studies of human RSV infection, including those focused on G, have been performed by directly exposing either airway epithelial or immune cells, but not both, to the virus. For example, human lung epithelial cells (A549) or primary normal bronchial epithelial cells have been used to study the production of proinflammatory and anti-inflammatory cytokines (interleukin-8 [IL-8], macrophage inflammatory protein-1 alpha (MIP-1α), MIP-1β, interferon-gamma inducible protein-10 (IP-10), monocyte chemoattractant protein 1 [MCP-1], and RANTES) upon infection with RSV lacking the G protein (29, 42). Human PBMCs directly stimulated with the purified RSV G protein produced significant levels of tumor necrosis factor alpha (TNF-α), IL-10, and IL-12 and became unresponsive to subsequent stimulation with the whole virus (43). Stimulation of human isolated monocytes with a peptide containing the CX3C region suppressed secretion of IL-6 and prevented facilitation of IL-6 and IL-1β responses upon subsequent exposure to endotoxin (lipopolysaccharide [LPS]) (32). However, a very limited number of studies have investigated the cross talk between RSV-infected airway cells and immune responses. A recent study by Qin et al. (44) employed a model of RSV infection consisting of a cocultured human airway epithelial cell line and PBMCs. RSV infection of airway cells efficiently induced T cell activation and the production of IFN-γ, IL-4, and IL-17 in PBMCs, although exposure of PBMCs to RSV-infected airway cells also accelerated apoptosis of lymphocytes. Coculture of PBMCs and airway cells, as used in the study by Qin et al., permits HLA-dependent reactions to occur, which could interfere with or confound RSV-associated responses. We chose to use a two-chamber system where A549 cells and PBMCs are separated by a permeable membrane. This system prevents contact between cells but permits exchange of viruses and viral and cellular proteins between the two chambers.

In the present study, we used the two-chamber *in vitro* model to characterize human innate and adaptive responses to RSV infection. We compared the responses of PBMCs exposed to A549 cells infected with RSV with either an intact CX3C motif (CX3C) or a mutated motif (CX4C) and also looked at the effect that the $F(ab')_2$ form of the anti-RSV G protein monoclonal antibody (MAb) 131-2G had on the infection. 131-2G binds to the conserved region of G and averts the RSV CX3C-CX3CR1 interaction (36). We demonstrate that elimination of the G protein interaction with CX3CR1 by using the CX4C virus or MAb 131-2G increased the innate and adaptive immune responses to RSV, i.e., prevented G-associated suppression of these immune responses.

MATERIALS AND METHODS

Cells. A549 cells, a human alveolar adenocarcinoma cell line (45), and HEp-2 cells were maintained in minimal essential medium (MEM) (Gibco, Invitrogen Corp., San Diego, CA) supplemented with 10% fetal bovine serum (FBS) (HyClone; Thermo Fisher Scientific, Inc., Suwanee, GA), penicillin-streptomycin, and L-glutamine at 37°C with 5% CO_2.

Viruses. Two RSV A2-derived strains, the wild type (wt) and the CX3C mutant (provided by A. G. P. Oomens), were generated with a reverse-genetic system as previously described (46). The wild-type strain (designated CX3C) has an intact CX3C motif (^{283}CWAIC^{287}) in the G protein and is the parent of the mutant strain (designated CX4C), which has an A^{286} insertion in the CX3C motif.

An RSV G open reading frame (ORF) with a mutated CX3C site was generated from an A2-based wt G ORF by site-directed mutagenesis. Three nucleotides (GCA) encoding an alanine residue were inserted before the second cysteine (C^{287}) to encode CWAIAC (G-CX4C) instead of the wt sequence, CWAIC (G-CX3C). To generate virus expressing G-CX4C and G-CX3C, an A2-based cDNA was constructed, which lacked the G ORF and contained instead a spacer with flanking BsmBI remote-cutting sites. Next, the G-CX4C and G-CX3C ORFs were PCR amplified to contain flanking BsmBI sites and cloned into the G-lacking RSV cDNA. The resulting cDNAs contained no artificial sequences or restriction sites other than the intended CX3C mutation and were used to recover viruses by reverse genetics. Viral genomes from passage 3 stocks were verified by harvesting of viral RNA from infected cells, amplification by real-time PCR (RT-PCR), and bulk sequence analysis.

Verified viral stocks underwent one passage in HEp-2 cells and were purified by pelleting through a 20% sucrose cushion at 16,000 × *g* for 2 h, resuspended in MEM without FBS, and stored at −80°C.

$F(ab')_2$ fragment preparation. MAb 131-2G $F(ab')_2$ fragments were generated by pepsin digestion (Sigma-Aldrich). Briefly, protein G column-purified MAb 131-2G (47) was digested with porcine pepsin overnight at 37°C, and digested MAb was passed through a protein G-Sepharose column (GE Healthcare, Alpharetta, GA) to eliminate Fc fragments and undigested antibodies. Purified $F(ab')_2$ fragments were dialyzed and concentrated by using a Centricon spin column (Millipore, Temecula, CA) with a 30-kDa cutoff. The purity of the $F(ab')_2$ fragments was determined by SDS-PAGE (Bio-Rad, Hercules, CA) under nonreducing conditions. The protein concentration was determined by a Micro BCA protein assay (Pierce Protein Research Products, Rockford, IL). Endotoxin concentrations were determined by using a *Limulus* amebocyte lysate chromogenic endpoint assay, in accordance with the manufacturer's instructions (Lonza, Atlanta, GA).

Mononuclear cell isolation. Peripheral blood from 8 random adult donors was collected under an Emory University institutional review board (IRB)-approved protocol and provided to the laboratory delinked from personal identifiers. PBMCs were isolated by centrifugation on a gradient of Ficoll-Paque Premium (GE Healthcare, Uppsala, Sweden). Briefly, blood was diluted 1:3 with phosphate-buffered saline (PBS), placed on top of the gradient, and centrifuged at 400 × *g* for 30 min at 21°C. Mononuclear cells were collected from the interface, washed 2 times with PBS, frozen in FBS containing 10% dimethyl sulfoxide (DMSO), and stored in liquid nitrogen until analysis.

***In vitro* model.** We used a two-chamber *in vitro* system (Fig. 1A) with the PBMCs in the upper chamber and A549 cells in the lower chamber to model RSV infection. A549 cells were grown in 24-well tissue culture plates and infected with CX3C or CX4C virus at a multiplicity of infection (MOI) of 0.01 or a comparable concentration of mock-infected cell culture medium (supernatants from uninfected HEp-2 cells prepared in the same manner as virus stocks). The virus inoculum was incubated for 2 h at 37°C and then replaced with fresh medium. Infected A549 cells were incubated for 3 days at 37°C under 5% CO_2, with fresh culture medium replacement on day 2 postinfection (p.i.), and PBMCs were then added as follows.

Freshly thawed PBMCs were resuspended in MEM–10% FBS, and live cells were counted by using trypan blue exclusion staining. PBMCs were diluted to 10×10^6 live cells/ml, and 100 μl (10^6 cells) was added to permeable polyester Transwell inserts (0.33 cm with a 0.4-μm pore size;

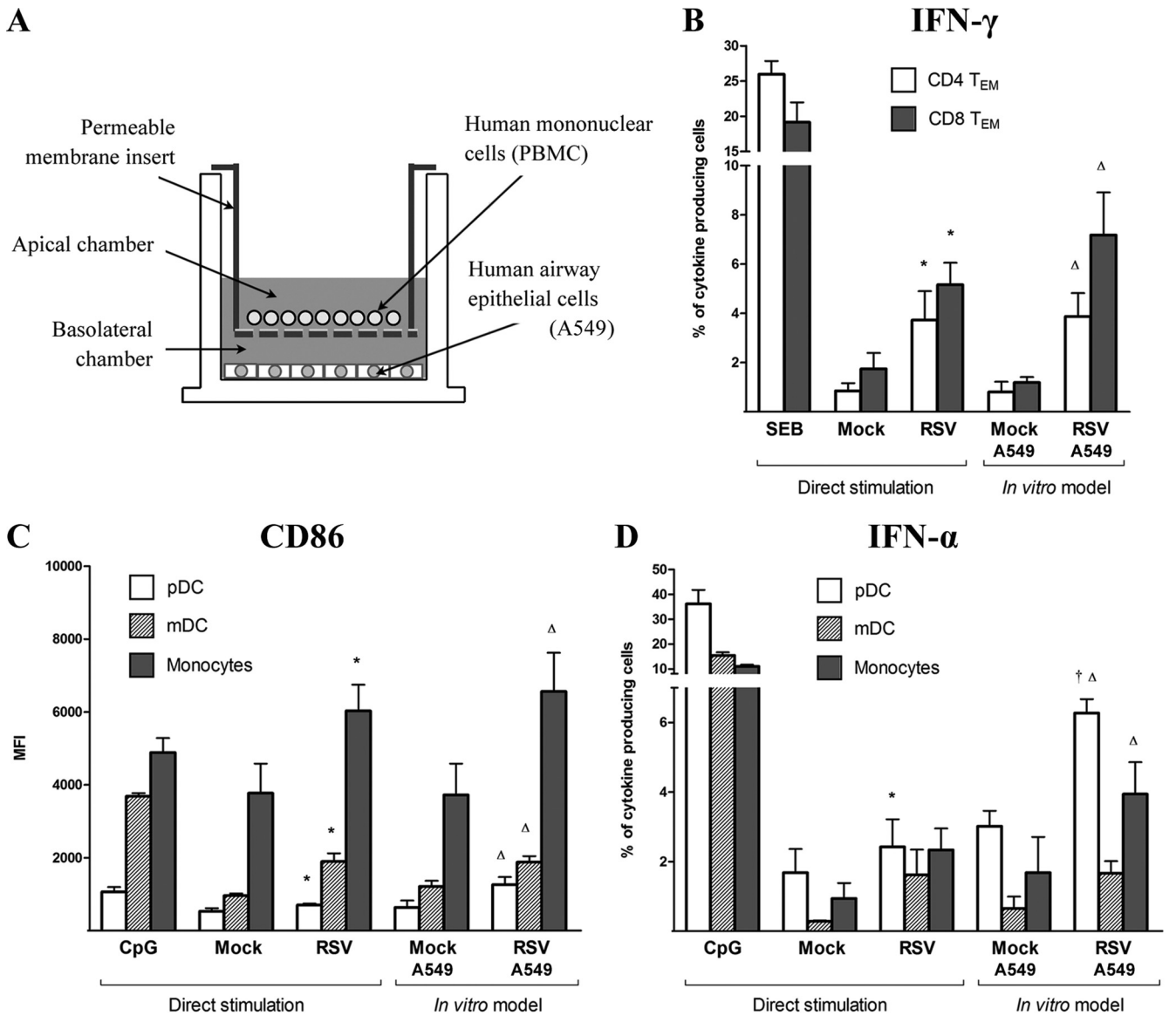

FIG 1 *In vitro* model of human RSV infection. (A) Human airway epithelial cells (A549) were cultured in 24-well plates and infected with RSV strains or mock infected and cultured for 3 days, with culture medium replacement on day 2 p.i. At day 3 p.i., PBMCs from random human adult donors were added in permeable-membrane Transwell inserts and coincubated for an additional 24 h. (B to D) Responses of PBMCs after exposure to purified CX3C RSV (direct stimulation) or RSV-infected A549 cells (*in vitro* model). Shown are the percentages of $CD69^+$ IFN-γ-producing CD4 and CD8 effector memory T cells (B), mean fluorescence intensity (MFI) of CD86 expression (C), and percentages of IFN-α-producing pDCs, mDCs, and monocytes (D). SEB or CpG was used as a positive control for T cell or innate cell responses. The data are represented as means ± SEM of independent experiments with PBMCs from 3 random donors. *, $P < 0.05$ versus mock infection in direct stimulation; △, $P < 0.05$ versus mock infection in the *in vitro* model; †, $P < 0.05$ versus direct stimulation (determined by a paired *t* test).

Corning, Inc., Corning, NY) in 24-well plates with 3-day-infected A549 cells and incubated for 24 h at 37°C under 5% CO_2. Wells without inserts were used to assess A549-produced cytokine responses without PBMCs.

In experiments with $F(ab')_2$ 131-2G, A549 cells were pretreated for 2 h with the MAb and then infected with CX3C or CX4C virus, incubated for 3 days, and coincubated with PBMCs for another 24 h, as stated above. $F(ab')_2$ 131-2G was added to the medium of A549 cells, the virus inoculum, and medium for PBMCs at a final concentration of 25 μg/ml. Mock-infected control A549 cells were treated in a similar fashion.

For the direct stimulation of PBMCs, freshly thawed cells were resuspended in RPMI–10% FBS and placed into a 96-well plate at 1×10^6 cells/well. CX3C virus (wild type) was added at a dose of 1 MOI, and the same amount of uninfected HEp-2 cell supernatant prepared in the same manner as the virus stock (mock) was added to control wells. PBMCs were incubated for 24 h at 37°C under 5% CO_2 and for an additional 2 h in the presence of brefeldin A (GolgiPlug; BD, San Jose, CA) and then processed in the same manner as the *in vitro*-coincubated PBMCs for the flow cytometric analysis (see below). As a positive control for IFN-α production, CpG oligonucleotide 2336 (human TLR9 ligand) was added at a final concentration of 2.5 μM. As a positive control for T cell cytokine production, staphylococcal enterotoxin B subunit (SEB) was added at a final concentration of 1 μg/ml.

RSV replication. The titer of infectious virus (50% tissue culture infectious dose [$TCID_{50}$]) was determined by a microtiter infectivity assay

using an enzyme-linked immunosorbent assay (ELISA) to detect virus replication, as previously described (48). Briefly, HEp-2 cells were grown in a 96-well microtiter plate, infected with 20 μl of 10-fold serial dilutions of the virus, and incubated for 2 h at room temperature (RT) with gentle rocking; 180 μl of medium was then added to each well; and the plate was incubated at 37°C under 5% CO_2 for 5 days. After the 5-day incubation, the wells were washed 3 times with PBS, fixed by incubation for 10 min at RT with 70% ethanol, dried, and stored at 4°C until testing. For the ELISA, cells were washed 4 times with PBS–0.5% Tween 20 (PBS-Tw), blocked for 1 h with PBS-Tw containing 5% bovine serum albumin (BSA), and then incubated for 2 h at 37°C with goat anti-RSV antibody (Millipore, Billerica, MA) diluted at 1:5,000. Next, wells were incubated for 1 h at 37°C with horseradish peroxidase (HRP)-conjugated donkey anti-goat antibody diluted at 1:5,000 (Jackson ImmunoResearch Laboratories, Inc., West Grove, PA), washed, and developed by using o-phenylenediamine (OPD) substrate. Absorbance was read at 490/640 nm.

The replication of viruses in A549 cells was measured similarly: Transwell inserts were removed, and supernatants in the lower chamber were collected and stored for testing. The cells remaining in the 24-well plates were then washed 3 times with PBS and fixed with 500 μl/well of 70% ethanol, and the plates were dried and stored at 4°C. The ELISA was performed directly in the 24-well plates as noted above, except with 3-fold greater volumes of reagents. After the color was developed and the reaction was stopped, supernatants were transferred onto a 96-well plate to read the absorbance.

The amount of viral RNA in the basolateral supernatants of RSV-infected and mock-infected A549 cells was determined by an RT-PCR assay. Total RNA was extracted from supernatants by using the Qiagen Total RNA extraction kit (Qiagen, Valencia, CA) according to the manufacturer's instructions and stored at −80°C. RT-PCR was performed by using an AgPath-ID OneStep RT-PCR kit (Applied Biosystems, Foster City, CA) and an ABI 7700 sequence detector system (Applied Biosystems, Foster City, CA). The thermal cycling conditions included 45°C for 2 min and 95°C for 10 min, followed by 40 cycles of amplification at 95°C for 15 s and 55°C for 2 min for denaturing and annealing, respectively. The primers and probes for the RSV matrix (M) gene (forward primer 5′-GGC AAA TAT GGA AAC ATA GCT GAA-3′, reverse primer 5′-TCT TTT TCT AGG ACA TTG TAY TGA ACA G-3′, and probe 5′–6-carboxyfluorescein [FAM]–TGT CCG TCT TCT ACG CCC TCG TC–black hole quencher 1 [BHQ-1]–3′), as previously described (49), were obtained from Integrated DNA Technologies. The cycle threshold (C_T) values, the number of cycles required to exceed the background level, were calculated.

Cytokine analysis. The supernatants from the lower chamber were harvested on day 3 p.i. (6 h after addition of inserts) and on day 4 p.i. (24 h after addition of inserts), stored at −80°C, and then tested for cytokine levels. For cytokine testing, the freshly thawed supernatants were centrifuged at 450 × *g* for 3 min to eliminate cell debris and analyzed by Luminex magnetic bead kits for IFN-α2, IFN-λ1 (IL-29), and IFN-λ2 (IL-28a) (Millipore). The assay was performed according to the manufacturer's instructions but with half the recommended quantity of beads, biotinylated antibody, and fluorescent dye-labeled streptavidin. Serial dilutions of standards for each analyte were used in each test to calculate the concentration of the analyte according to the manufacturer's instructions.

Flow cytometric analysis of PBMCs. PBMCs were harvested from the Transwell inserts after 24 h of coincubation with RSV or mock-infected A549 cells (as noted above). Cells were transferred from inserts into separate wells in a 96-well plate. Residual cells on the insert were acquired by washing the inserts 2 times with Versene (0.48 mM EDTA) solution (Gibco, Invitrogen), with 5 min of incubation at 37°C during each washing step. The cells were centrifuged at 450 × *g* for 3 min and resuspended in 200 μl of the original supernatant, to which brefeldin A (BD GolgiPlug) was added and incubated for 2 h at 37°C under 5% CO_2. The cells were then washed 2 times with staining buffer (BD Pharmingen), stained with Live/Dead fixable red dye (Invitrogen), incubated for 1 h at 4°C with TruStain (BioLegend, Inc., San Diego, CA) to block Fc receptors to decrease nonspecific staining, and stained for 30 min at 4°C with two panels of fluorochrome-labeled antibodies, one to test for innate (monocytes/dendritic cells) responses and one to test for memory/effector T (T_{EM}) cell responses.

The innate response panel consisted of antibodies against CD3, CD19, and CD56 (Brilliant Violet 570; BioLegend); CD14 (allophycocyanin [APC]-Cy7; BioLegend); HLA-DR (V500; BD Horizon); CD11c (Alexa Fluor 700; eBioscience, Inc., San Diego, CA); CD303a (fluorescein isothiocyanate [FITC]; eBioscience); and CD86 (phycoerythrin [PE]-Cy7; BioLegend). Monocytes and dendritic cells were analyzed after excluding dead cells within the $CD3^-$ $CD19^-$ $CD56^-$ subpopulation as $CD14^+$ $HLA\text{-}DR^+$ monocytes, $CD14^-$ $HLA\text{-}DR^+$ $CD11c^+$ $CD303a^-$ myeloid dendritic cells (mDCs), and $CD14^-$ $HLA\text{-}DR^+$ $CD11c^-$ $CD303a^+$ plasmacytoid dendritic cells (pDCs). The activation and maturation status of the cells was determined by staining for surface expression of CD86 and HLA-DR. Cytokine production was assessed by intracellular staining as previously described (50). Briefly, after surface staining, the cells were washed 2 times with staining buffer, fixed for 10 min at RT with BD fluorescence-activated cell sorter (FACS) lysing solution, washed, permeabilized for 10 min at RT with BD FACS permeabilization solution 2, washed, and incubated for 30 min at 4°C with fluorochrome-labeled antibodies against IFN-α2b (V450; BD Horizon), TNF-α (PE; eBioscience), and MCP-1 (APC; eBioscience).

The memory/effector T cell panel consisted of antibodies against CD3 (eFluor 605NC; eBioscience), CD4 (APC-H7; BD Biosciences), CD8 (V500; BD Horizon), CD45RA (Alexa Fluor 700; BioLegend), CCR7 (PE-Cy7; BD Pharmingen), and CD69 (APC; BioLegend). Memory/effector T cells were analyzed after excluding dead cells within $CD3^+$ CD4/CD8 subpopulations as $CD45RA^-$ $CCR7^+$ central memory T (T_{CM}) cells and $CD45RA^-$ $CCR7^-$ T_{EM} cells and only within the $CD8^+$ subpopulation as $CD45RA^+$ $CCR7^-$ effector T cells expressing CD45RA (T_{EMRA} cells). The activation and functional status of T cells were determined by surface expression of CD69 and production of cytokines. Intracellular cytokine staining was performed in the same manner as for monocytes and dendritic cells; i.e., cells were stained with fluorochrome-labeled antibodies against IFN-γ (FITC; BioLegend) and IL-4 (PE; BioLegend).

Flow cytometry analysis was performed by using a 4-laser BD LSR-II instrument (BD Biosciences) and FlowJo software (Tree Star, Inc., Ashland, OR).

Data analysis. Statistical analysis and graphs were performed by using GraphPad Prism software (GraphPad Software, Inc., La Jolla, CA). Data are expressed as means ± standard errors of means (SEM) of independent experiments with PBMCs from 5 random donors [3 donors for $F(ab')_2$ 131-2G experiments] and 3 replicates for each experimental condition. The Wilcoxon matched-pairs test was employed to determine the significance of differences between CX3C RSV, CX4C RSV, and mock infections. The Mann-Whitney test was used for comparison of the different viruses and mock-infected A549 cells without PBMCs. A P value of <0.05 was considered to be statistically significant.

RESULTS

***In vitro* model of human RSV infection.** To study human airway and immune cell responses to RSV, we developed a two-chamber *in vitro* system comprised of human A549 cells and PBMCs separated by a permeable membrane (Fig. 1A). The system prevents direct cell-to-cell interaction but allows exchange of virus, viral proteins, and cellular mediators between the two chambers, i.e., cross talk between immune and airway epithelial cells.

To characterize this *in vitro* model, we examined the kinetics of RSV replication and cytokine responses in A549 cells and compared the response of PBMCs exposed to RSV-infected A549 cells to that of PBMCs exposed to purified RSV. The kinetics of RSV infection in A549 cells (data not shown) showed that day 3 p.i. was

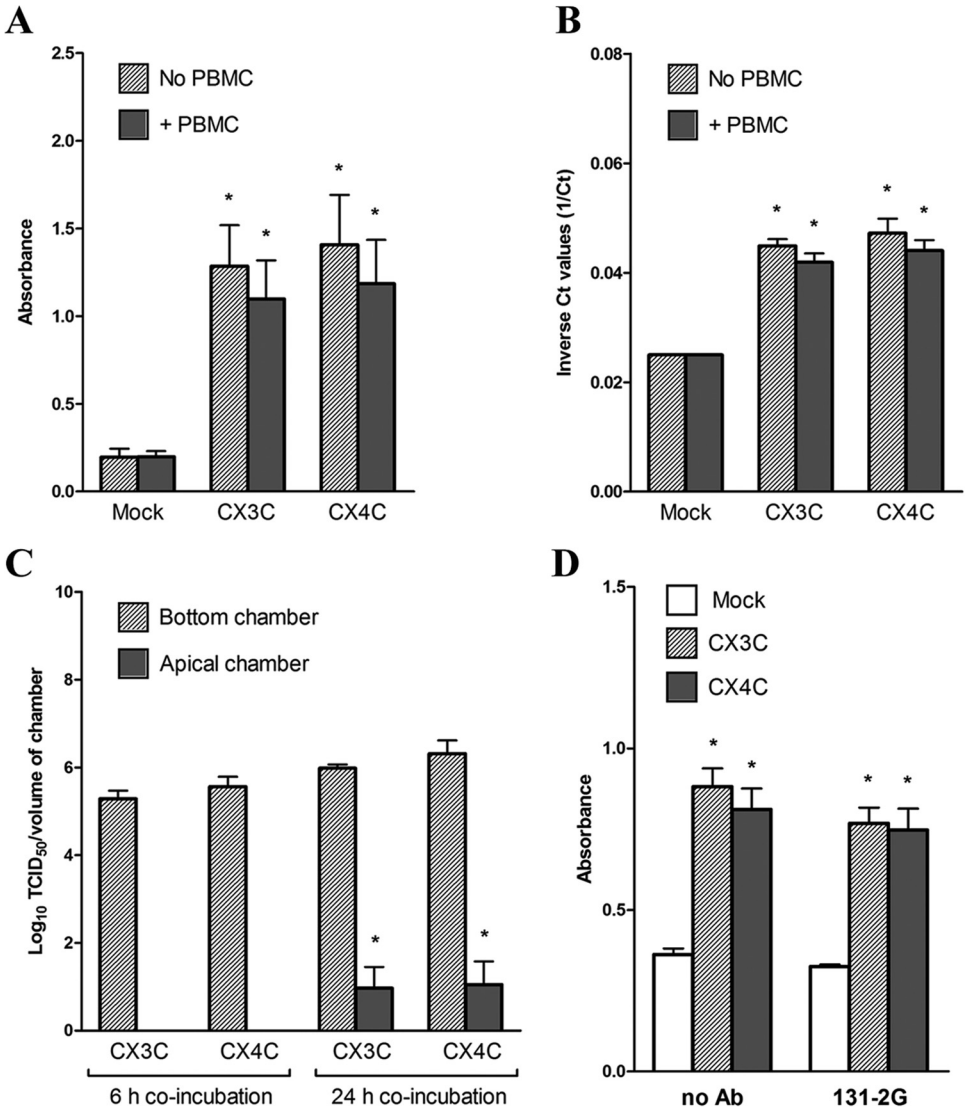

FIG 2 Replication of wild-type RSV (CX3C) and mutant RSV with an altered CX3C motif of the G protein (CX4C) in the *in vitro* model of human RSV infection. (A) Virus replication in A549 cells, determined by RSV-specific ELISA. A549 cells were infected and incubated for 3 days, with culture medium replacement on day 2 p.i. At day 3 p.i., PBMCs from random human adult donors were added in permeable-membrane inserts and coincubated for an additional 24 h. After coincubation and removal of the inserts and supernatants, A549 cells were washed and fixed, and an RSV-specific ELISA was performed. Absorbance represents the amount of surface and internal RSV antigens captured by ELISA. The data are represented as means ± SEM of independent experiments with PBMCs from 5 random donors. *, $P < 0.05$ versus mock infection (determined by the Mann-Whitney test). (B) Relative amount of viral RNA in basolateral supernatants of infected A549 cells determined by RT-PCR, represented as inverse cycle threshold (C_T) values. C_T levels reflect the number of cycles required to exceed the background level; inverse C_T levels ($1/C_T$) are proportional to the amount of target nucleic acid in the sample. RT-PCR underwent 40 cycles of amplification. The data are represented as means ± SEM of independent experiments with PBMCs from 5 random donors. (C) Viral titers in the bottom and top chambers after 6 or 24 h of coincubation of PBMCs with infected A549 cells, determined by a microtiter tissue culture infectivity assay. The data are represented as means ± SEM of 3 repeated independent experiments with PBMCs from one random donor. Mononuclear cells were coincubated with RSV-infected A549 cells. *, $P < 0.05$ versus the bottom chamber (determined by the Mann-Whitney test). (D) RSV-specific ELISA of A549 cells infected with CX3C and CX4C viruses with or without the presence of $F(ab')_2$ fragments of monoclonal anti-G protein 131-2G antibody. Absorbance represents the amount of surface and internal RSV antigens detected by ELISA. The data are represented as means ± SEM of independent experiments with PBMCs from 3 random donors. *, $P < 0.05$ versus mock infection (determined by the Mann-Whitney test).

the first day with consistent, detectable replication of virus and RSV-associated increases in levels of cytokines and chemokines. We chose day 3 p.i. to add PBMCs to the infected A549 cells. By day 4 p.i., the titers of infectious virus ($TCID_{50}$) in supernatants were $\approx 1 \times 10^6$ (range, 8.0×10^5 to 1.3×10^6). To compare direct stimulation of PBMCs with RSV to stimulation with RSV-infected A549 cells, we used the same donor PBMCs, the same time of incubation (24 h), and the same inoculum (1×10^6 $TCID_{50}$) of the purified wild-type CX3C strain of RSV. We determined the intracellular production of IFN-γ (Fig. 1B) and IL-4 (data not shown) to assess responses in CD4 and CD8 T_{EM} cells and the expression of the maturation marker CD86 (Fig. 1C) and intracellular IFN-α (Fig. 1D) and MCP-1 (data not shown) to assess responses in dendritic cells and monocytes.

TABLE 1 Estimated effect of differences in virus replication on response values

PBMC donor	Virus replication (RSV ELISA absorbance)		Difference in RSV ELISA absorbance	Estimated difference in response values associated with difference in RSV ELISA absorbance			
	CX3C	CX4C		IFN-λ1 in A549 cells (pg/ml)	IFN-α-producing pDCs (%)	TNF-α-producing pDCs (%)	IFN-γ-producing CD8 T_{EM} cells (%)
0801	0.946	0.744	0.202	3,201	0.18	1.09	0.57
0928	1.020	0.751	0.269	10,397	0.95	1.40	1.09
0930	0.871	1.091	0.220	6,434	0.36	1.17	0.71
1023	1.702	1.972	0.270	10,505	0.96	1.41	1.10
1046	0.930	1.218	0.288	11,738	1.17	1.49	1.24

Stimulation of PBMCs with purified RSV or RSV-infected A549 cells gave a similar pattern of responses, although exposure to RSV-infected A549 cells induced higher levels of innate immune responses. The percentages of IFN-α-producing pDCs and MCP-1-producing mDCs were significantly higher in PBMCs exposed to RSV-infected A549 cells than in PBMCs stimulated with purified virus. Although the average percentages of IFN-α-producing monocytes, IFN-γ-producing CD8 T_{EM} cells, and IL-4-producing CD4 T_{EM} cells were higher for PBMCs exposed to infected A549 cells, the difference compared to purified virus stimulation did not reach statistical significance. The control responses of the PBMCs exposed to the mock-infected cells were similar to the responses of directly mock-stimulated PBMCs, showing that uninfected A549 cells do not induce PBMC responses.

These findings indicate that our *in vitro* system of exposing PBMCs to RSV-infected A549 cells effectively detects responses and may be especially suited to studies of innate immune responses.

Altering the CX3C site does not affect virus replication in A549 cells. A549 cells were infected with two RSV strains: the wild type (CX3C), containing an intact CX3C motif in the G protein, or a mutant virus (CX4C), with an additional alanine preceding the second cysteine. Both RSV strains had similar replication rates in human A549 cells, as indicated by the amount of RSV antigens detected by ELISA (Fig. 2A) and the relative amount of viral RNA detected by real-time PCR (Fig. 2B). The addition of PBMCs to A549 cells on day 3 p.i. was associated with a minor decrease in viral replication for both viruses. Thus, mutating the CX3C site did not impact RSV replication in A549 cells. We also noted that the virus did slowly cross the membrane, as evident by the lack of infectious virus in the upper chamber at 6 h and the presence of low levels at 24 h after the addition of the PBMCs (Fig. 2C), as would be expected with a 0.4-μm pore diameter. The addition of $F(ab')_2$ fragments of 131-2G to the cells (Fig. 2D) slightly decreased the levels of replication for both viruses. It appeared that the MAb affected the CX3C virus more than the CX4C strain, reducing the difference in replication between the two viruses; these effects, though, were not statistically significant.

To minimize the effect that differences in virus replication might have on responses, we used an inoculum of the virus that gave similar levels of replication for the two viruses at the study

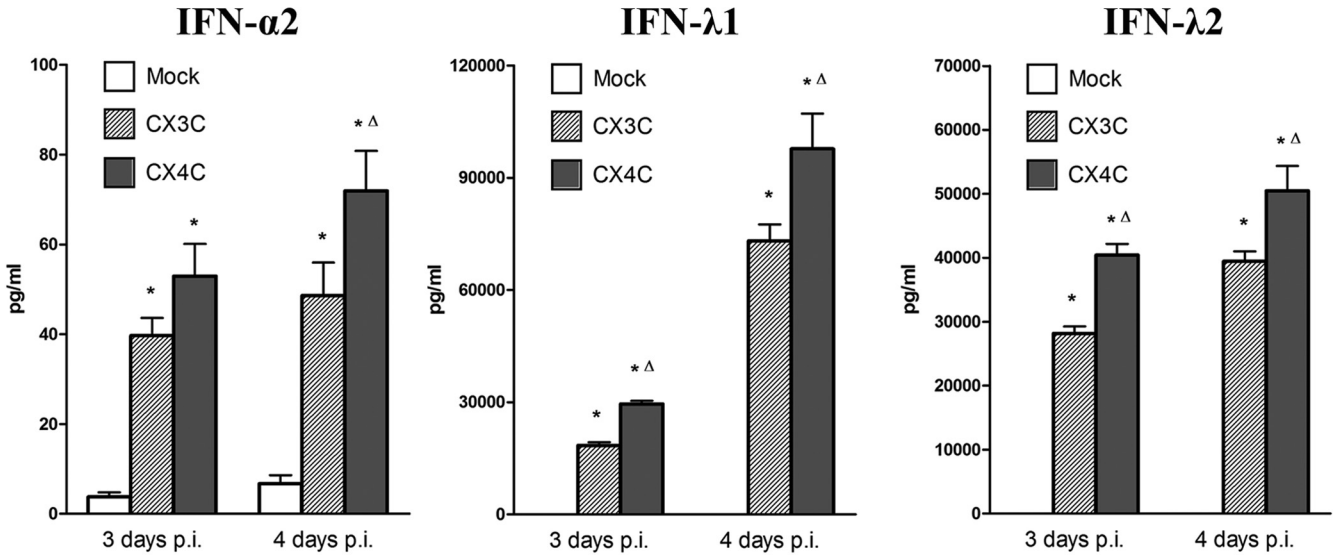

FIG 3 Antiviral responses of A549 cells infected with wild-type RSV (CX3C) and mutant RSV with an altered CX3C motif of the G protein (CX4C). A549 cells were mock infected or infected with the CX3C or CX4C RSV strain and incubated for 4 days, with culture medium changed on day 2 postinfection. Supernatants from the bottom chamber were collected on days 3 and 4 postinfection (6 h and 24 h after addition of inserts, respectively). The Luminex assay was performed with collected supernatants to measure production of IFN-α2, IFN-λ1, and IFN-λ2. The data are represented as means ± SEM of 3 repeated independent experiments. *, $P < 0.05$ versus mock infection; △, $P < 0.05$ versus CX3C (determined by the Mann-Whitney test).

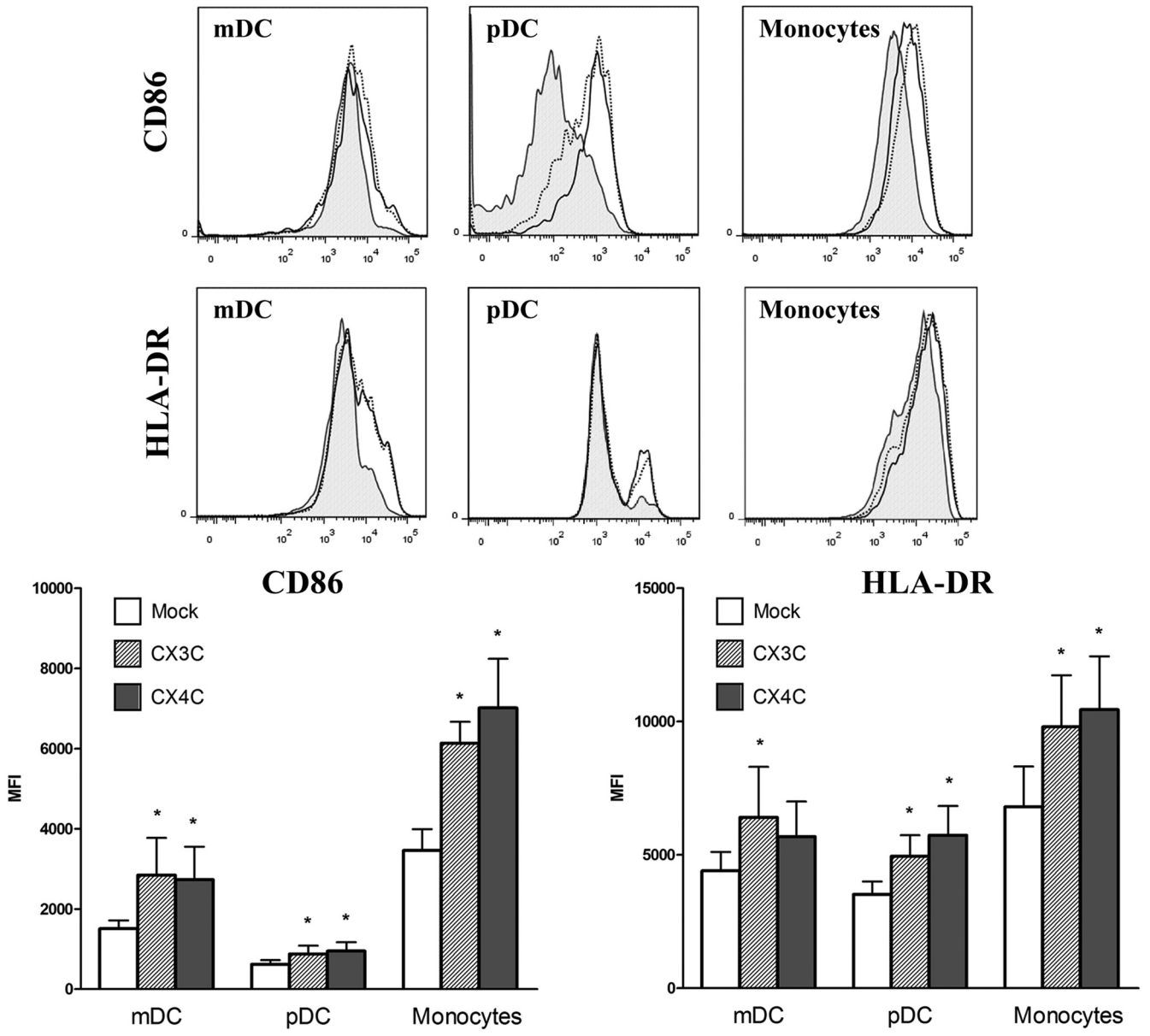

FIG 4 Activation/maturation of human dendritic cells and monocytes during coincubation with RSV CX3C- or CX4C-infected A549 cells. Histograms show expression of HLA-DR and the costimulatory molecule CD86 on the surface of single-donor PBMCs coincubated for 24 h with A549 cells that were mock infected (gray area) or infected with CX3C (solid lines) and CX4C (dotted lines) RSV strains. Graphs show the geometric mean fluorescence intensity (MFI) of CD86 and HLA-DR expressed on myeloid (mDC) and plasmacytoid (pDC) dendritic cells and monocytes. The data are represented as means ± SEM of independent experiments with PBMCs from 5 random donors. *, $P < 0.05$ versus mock infection (determined by the Wilcoxon matched-pairs test).

time points. However, experimental variation left some differences in levels of virus replication. To determine the effect of these differences on our results, we calculated the estimated values of responses by interpolating from a standard curve of virus replication (RSV antigen-specific ELISA absorbance) versus the response measure values for both viruses. One set of PBMCs was used to generate the standard curve. Table 1 shows the individual replication results for each PBMC set, the difference in levels of replication between the two viruses observed for each experiment, and examples of the estimated change in response values associated with the difference in replication.

Virus replication had unequal effects on the responses measured. For example, virus replication had a greater impact on the percentage of TNF-α than IFN-α-producing pDCs or IFN-γ-producing CD8 T_{EM} cells, as the estimated values of responses were higher for TNF-α-producing dendritic cells (Table 1). To estimate this influence on differences in responses between CX3C and CX4C viruses, we normalized the original data to replication of both viruses using the estimated response values from the standard curve.

The CX3C motif alters antiviral responses in A549 human airway epithelial cells. To study innate antiviral responses in A549 cells, we measured the production of IFN types I and III in response to infection with CX3C and CX4C viruses (Fig. 3). Newly

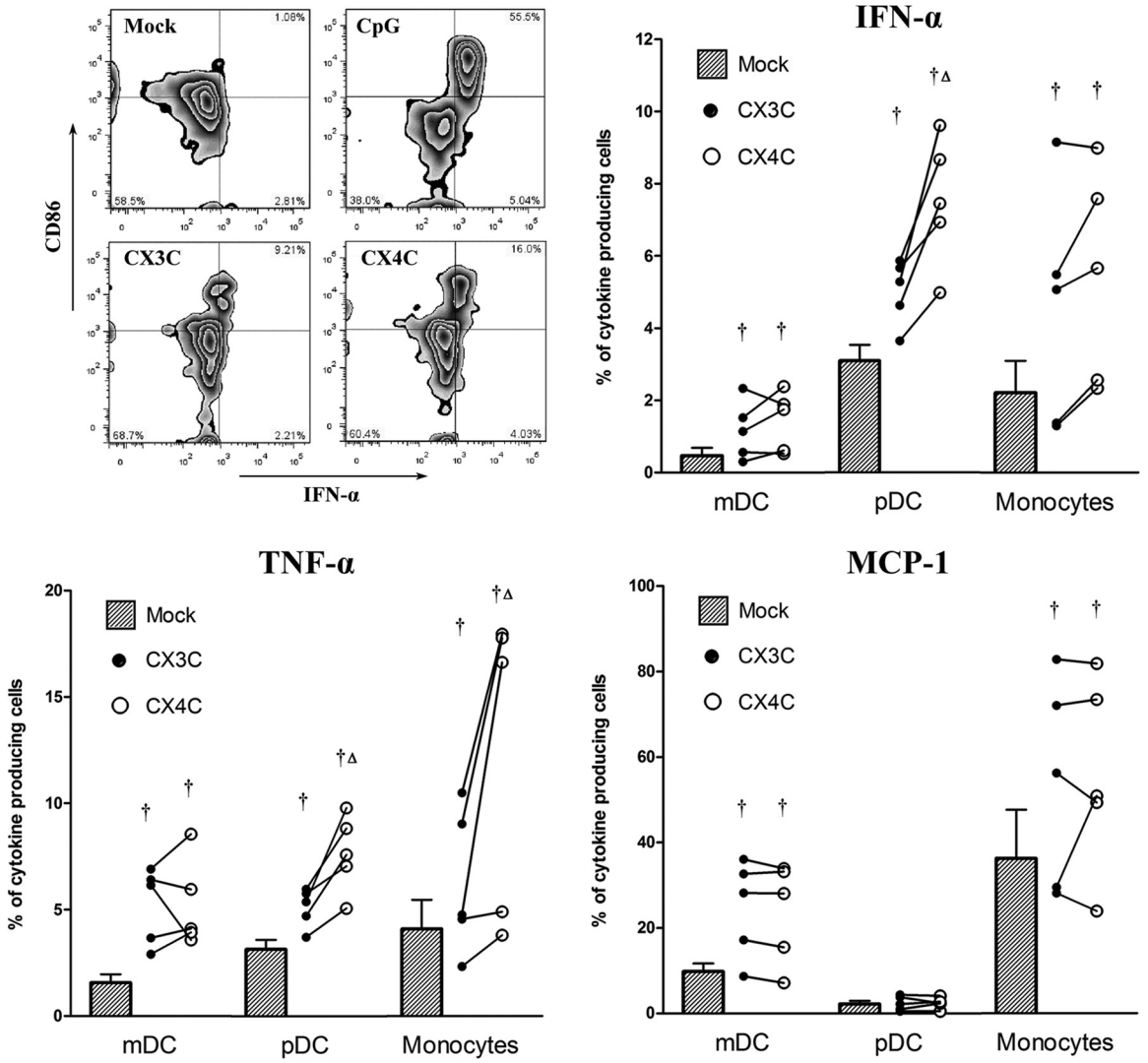

FIG 5 Innate immune responses of human PBMCs coincubated with A549 cells infected with CX3C or CX4C virus. A549 cells were mock infected or infected with the CX3C or CX4C RSV strain and cultured for 3 days, with culture medium replacement on day 2 p.i. and addition of PBMCs in permeable-membrane inserts on day 3 p.i. After coincubation for an additional 24 h, PBMCs were harvested and analyzed. The counterplot shows the distribution of plasmacytoid dendritic cells expressing CD86 and intracellular IFN-α (data for PBMCs from a single donor). CpG (ODN 2336), a human TLR9 ligand, was used as a positive control for IFN-α production. Graphs show the percentages of myeloid (mDC) and plasmacytoid (pDC) dendritic cells and monocytes producing IFN-α, TNF-α, and MCP-1. The data are represented as means ± SEM of independent experiments with PBMCs from 5 random donors and individual paired results for each donor. †, $P < 0.05$ versus mock infection; △, $P < 0.05$ versus CX3C (determined by the Wilcoxon matched-pairs test).

identified type III IFNs have antiviral activity like type I IFNs (51), and although type I and type III IFN receptors are unrelated, they trigger similar Jak-STAT signaling pathways (52, 53).

RSV infection of A549 cells induced both IFN-α2 and IFN type III (IFN-λ1/2) on day 3 p.i. and day 4 p.i. Both viruses induced approximately 400- to 1,000-times-higher levels of IFN type III (11,430 to 78,940 pg/ml of IFN-λ1 and 26,550 to 42,350 pg/ml of IFN-λ2) than of IFN type I (27 to 72 pg/ml of IFN-α2). Interestingly, the CX4C virus induced even higher levels of both IFN types I and III. The levels of IFN-λ1 and -λ2 were significantly higher for the CX4C virus than for the CX3C virus on both day 3 and day 4 p.i., while the IFN-α2 levels were significantly higher only on day 4 p.i. Normalization of responses to virus replication did not change the pattern or significance of differences seen with the original data. Thus, RSV with an intact G protein CX3C motif appears to suppress antiviral responses in A549 cells.

Altering the CX3C site does not decrease activation/maturation of dendritic cells and monocytes. After 24 h of exposure to RSV-infected A549 cells, PBMCs were harvested from the inserts and stained with fluorochrome-labeled antibodies to distinguish mDCs, pDCs, and monocytes. The activation/maturation state of dendritic cells and monocytes was assessed by the expression of the costimulatory molecule CD86 and the increased expression of major histocompatibility complex class II (MHC-II) (HLA-DR) (Fig. 4). CD86 (B lymphocyte/accessory cell activation antigen B7-2) is a ligand for T cell-costimulatory CD28/cytotoxic-T lymphocyte-associated antigen 4 (CTLA-4) molecules, provides costimulatory signals necessary for T cell activation, and appears

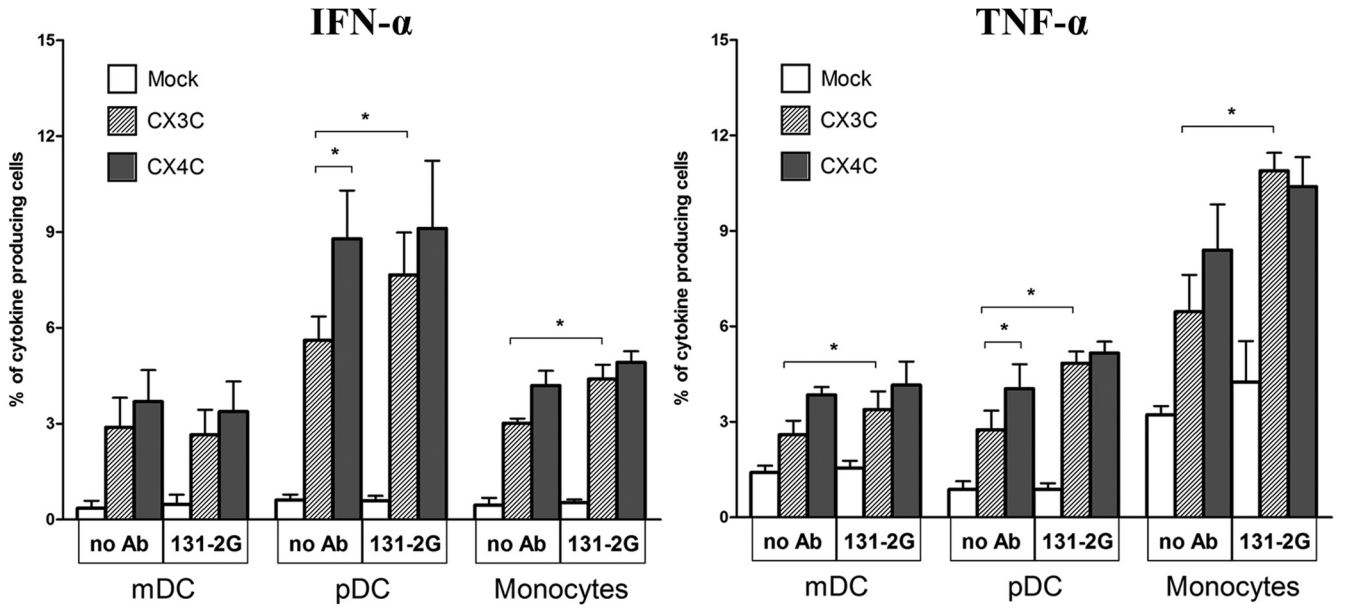

FIG 6 Innate immune responses of human PBMCs coincubated with A549 cells infected with CX3C or CX4C virus in the presence of $F(ab')_2$ fragments of anti-G protein antibody. A549 cells were mock infected or infected with the CX3C or CX4C RSV strain and cultured for 3 days, with culture medium replaced on day 2 p.i. and PBMCs added to the permeable-membrane inserts on day 3 p.i. For the $F(ab')_2$-treated wells, A549 cells were pretreated with $F(ab')_2$ 131-2G MAb for 2 h before infection, and MAbs were included in medium changes and medium for the PBMCs. The PBMCs were harvested 24 h after exposure to A549 cells and studied by flow cytometry. Graphs show the percentages of myeloid (mDC) and plasmacytoid (pDC) dendritic cells and monocytes producing IFN-α and TNF-α. The data are represented as means ± SEM of independent experiments with PBMCs from 3 random donors. *, $P < 0.05$ (determined by the Wilcoxon matched-pairs test).

on the surface of dendritic cells and monocytes/macrophages after their transformation into fully efficient antigen-presenting cells (54, 55).

Exposure of PBMCs to RSV-infected A549 cells increased the surface density of CD86 and HLA-DR on both dendritic cells and monocytes for all donors. The wild-type and CX4C viruses had similar effects, suggesting that altering the CX3C motif in the RSV G protein does not change innate immune cell activation and maturation.

The CX3C motif impairs innate antiviral responses in pDCs. Plasmacytoid DCs are a major source of type I IFN and, as well as mDCs and monocytes, exhibit strong proinflammatory response to the antigens (56–58). In order to evaluate the impact of the RSV CX3C motif on the functionality of innate immune cells, we assessed cytokine production in dendritic cells and monocytes within PBMCs exposed to RSV-infected A549 cells.

In our *in vitro* model, both viruses induced significant increases in percentages of IFN-α-, TNF-α-, and MCP-1-producing monocytes and mDCs and percentages of IFN-α- and TNF-α-producing pDCs for most donor PBMCs (Fig. 5). We also found that the CX4C virus induced significantly higher percentages of IFN-α- and TNF-α-producing pDCs and TNF-α-producing monocytes. There were, however, no significant differences between the two viruses in percentages of cytokine-producing mDCs. Normalization of the data to virus replication had a slight effect on the differences in responses between the two viruses that did not change the statistical significance obtained with the original percentages of IFN-α-producing pDCs and TNF-α-producing monocytes. The normalized percentages of TNF-α-producing pDCs had a pattern similar to the original data, but the difference between CX3C and CX4C virus-exposed PBMCs was no longer significant.

The addition of $F(ab')_2$ fragments of anti-G protein MAb during CX3C infection increased the production of IFN-α and TNF-α in pDCs and monocytes (Fig. 6) to levels similar to those with the CX4C virus. The response of the CX4C virus was not significantly changed by addition of the MAb. These findings suggest that the intact CX3C motif downregulates the human innate immune response associated with IFN-α and TNF-α production in pDCs and monocytes.

The CX3C motif diminishes adaptive antiviral responses of CD4/CD8 T cells. In addition to innate immune responses, we tested effector/memory responses in CD4/CD8 T cell subpopulations. Three effector/memory T cell subsets were characterized by the expression of the homing receptor CCR7 and the CD45 naive isoform CD45RA, i.e., central memory (T_{CM}), effector memory (T_{EM}), and $CD45RA^+$ effector memory (T_{EMRA}) T cells (59). The T_{EMRA} cells typically belong to the CD8 subset (59). The few $CCR7^-$ $CD45RA^+$ (T_{EMRA} phenotype) CD4 T cells that could be distinguished (60) were, in our gating strategy, included in the CD4 T_{EM} subpopulation.

CD4 and CD8 effector and memory T cells from PBMCs from the 5 donors exposed to RSV-infected A549 cells responded with significant increases in percentages of activated CD69-positive IFN-γ- and IL-4-producing cells (Fig. 7). The CX4C virus induced a significantly higher percentage of IFN-γ-producing cells in CD4 T_{CM}, CD8 T_{EM}, and T_{EMRA} subpopulations than the CX3C virus. The percentage of IFN-γ-producing CD4 T_{EM} and CD8 T_{CM} cells after CX4C exposure was also higher, but the difference did not reach statistical significance. Notably, normalization of the data to virus replication did not affect the pattern or statistical significance observed with the original percentages of IFN-γ-producing memory T cells.

In contrast to IFN-γ responses, the numbers of IL-4-produc-

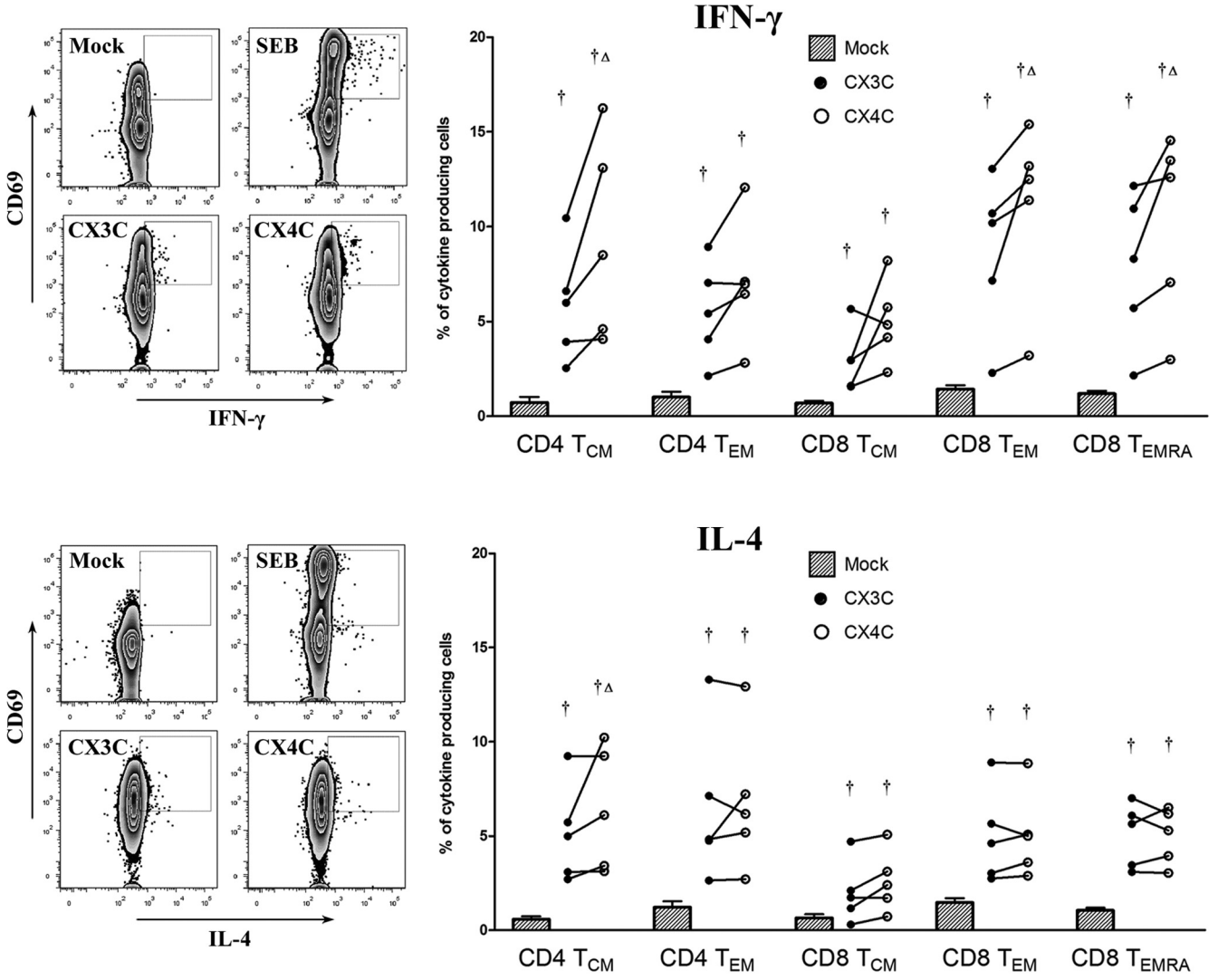

FIG 7 Memory T cell responses of human PBMCs coincubated with A549 cells infected with CX3C or CX4C virus. A549 cells were mock infected or infected with the CX3C or CX4C RSV strain and cultured for 3 days, with culture medium replacement on day 2 p.i. and addition of PBMCs in permeable-membrane inserts on day 3 p.i. After coincubation for an additional 24 h, PBMCs were harvested and analyzed. Counterplots show the distribution of CD8 effector memory T cells expressing CD69 and intracellular IFN-γ and of CD4 central memory T cells expressing CD69/IL-4. SEB was used as a positive control for IFN-γ/IL-4 production. Graphs show the percentages of $CD69^+$ central memory (T_{CM}), effector memory (T_{EM}), and $CD45RA^+$ effector memory (T_{EMRA}) T cells producing IFN-γ and IL-4. The data are represented as means ± SEM of independent experiments with PBMCs from 5 random donors and individual paired results for each donor. †, $P < 0.05$ versus mock infection; △, $P < 0.05$ versus CX3C (determined by the Wilcoxon matched-pairs test).

ing cells were similar between PBMCs exposed to wild-type-infected and those exposed to CX4C virus-infected A549 cells, except for the CD4 T_{CM} subpopulation, where 3 of 5 tested PBMC samples had a significantly higher percentage of IL-4-expressing cells after exposure to the CX4C virus than after exposure to the wild-type strain. After normalization to virus replication, the difference in the percentages of IL-4-producing CD4 T_{CM} cells between the two viruses no longer reached statistical significance.

The addition of $F(ab')_2$ anti-G MAb during CX3C infection gave results similar to those with CX4C virus with or without the MAb, i.e., higher percentages of IFN-γ-producing CD4 T_{CM}, CD8 T_{EM}, and T_{EMRA} subpopulations (Fig. 8), and support our findings with the CX3C and CX4C viruses. Overall, these data indicate that the RSV G protein CX3C motif downregulates adaptive immune responses, particularly the production of IFN-γ in effector/memory T cell subsets.

DISCUSSION

The G protein is recognized as being a substantial contributor to the RSV-induced host response to infection (61). It also appears that the G protein CX3C chemokine motif in particular contributes to some of these effects in mice (36, 40, 41). Our data obtained in an *in vitro* model of the human immune responses to RSV show that the CX3C motif is also likely relevant to both innate and adaptive immune responses during human RSV infection.

Three studies directly link the CX3C motif to RSV disease. In one study, FI-RSV-vaccinated mice which were challenged with RSV that had a deletion of the G gene or that had a Cys-to-Arg mutation at the CX3C motif (CX3R) or were pretreated with anti-

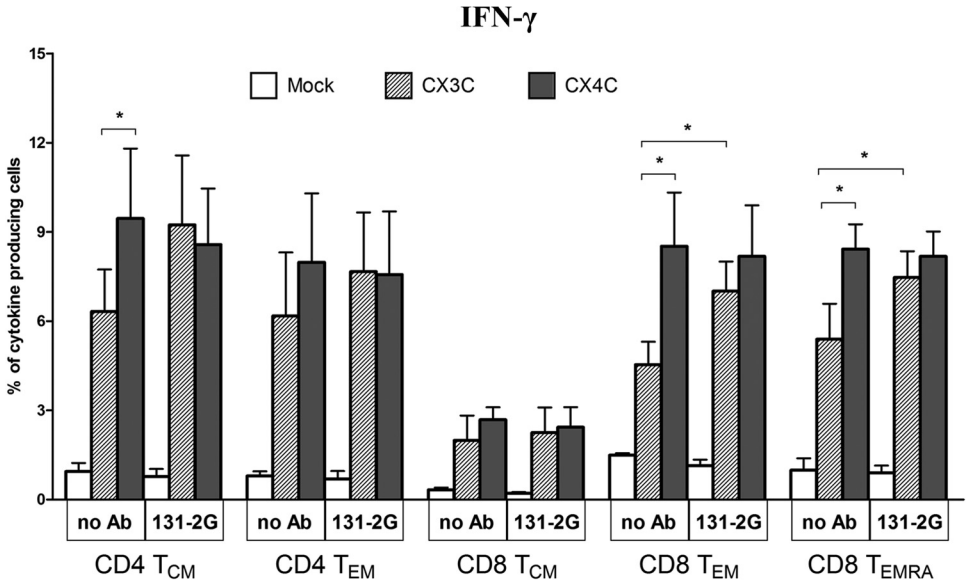

FIG 8 Memory T cell responses of human PBMCs coincubated with A549 cells infected with CX3C or CX4C virus in the presence of F(ab′)$_2$ fragments of anti-G protein antibody. A549 cells were mock infected or infected with the CX3C or CX4C RSV strain and cultured for 3 days, with culture medium replaced on day 2 p.i. and PBMCs added to the permeable-membrane inserts on day 3 p.i. For the F(ab′)$_2$-treated wells, A549 cells were pretreated with F(ab′)$_2$ 131-2G MAb for 2 h before infection, and MAbs were included in medium changes and medium for the PBMCs. The PBMCs were harvested 24 h after exposure to A549 cells and studied by flow cytometry. The graph shows the percentages of CD69$^+$ central memory (T$_{CM}$), effector memory (T$_{EM}$), and CD45RA$^+$ effector memory (T$_{EMRA}$) T cells producing IFN-γ. The data are represented as means ± SEM of independent experiments with PBMCs from 3 random donors. *, $P < 0.05$ (determined by the Wilcoxon matched-pairs test).

CX3CR1 antibody had marked decreases in the enhanced pulmonary inflammation otherwise seen in FI-RSV-vaccinated mice (41). In another study, mice challenged with the RSV CX3R mutant had significantly higher levels of effector T cell trafficking into inflamed lungs and T cell production of IFN-γ/IL-4 than mice challenged with wild-type RSV (40). In the third study, mice given the RSV G protein intravenously had a decreased respiratory rate, but mice given the CX3R mutant G or anti-CX3CR1 antibody before administration of the G protein did not experience a decrease in the respiratory rate (36).

All three studies showing a role of the CX3C-CX3CR1 interaction in host immune responses were performed with the murine system. Our data using the two-chamber *in vitro* RSV infection model identified CX3C effects on both the innate and adaptive responses in human cells. The differences between intact (CWAIC) and mutated (CWAIAC) CX3C motifs suggest a significant effect on both antiviral and inflammatory innate responses. To assess antiviral responses in human airway epithelial cells, we tested the production of both type I and type III IFNs in RSV-infected A549 cells. The newly characterized IFN type III includes IFN-λ1, -λ2, and -λ3 (52, 62), and its production occurs primarily in epithelial cells (63–65). Okabayashi et al. suggested that production of IFN-λ, but not IFN type I, is the primary antiviral defense against RSV infection in normal bronchial epithelial cells (66). Similarly, we found that RSV infection of A549 cells induced much higher levels of IFN-λ than of IFN-α (Fig. 3). Low-level or absent production of IFN-α by RSV-infected airway epithelial cells (primary cultures) has been well documented (67, 68). RSV appears to effectively suppress the host IFN-α/β responses by the expression of the nonstructural proteins NS1 and NS2 (69–71). In addition, the RSV attachment G protein has also been suggested to suppress type I IFN responses by reducing the expression levels of the cytokine-signaling SOCS3 protein and the interferon-stimulated gene ISG15 (72). Our data show significant increases in levels of IFN-λ1 and -λ2 in A549 cells infected with the CX4C virus (Fig. 3B and C), suggesting that the CX3C chemokine motif contributes to the suppression of IFN production. We found that A549 cells express fairly low levels of CX3CR1 (less than 1% of total cells [data not shown]). This low expression level of CX3CR1 in A549 cells appears to be sufficient to affect IFN type I/III production but not high enough to significantly increase infection (Fig. 2).

Our *in vitro* model allows us to also look at the effect of RSV-infected airway cells on immune cell responses. We found that the presence of PBMCs did not significantly affect virus replication, while the membrane allowed virus to pass through (Fig. 2). The microenvironment of RSV-infected A549 cells induced a variety of responses in PBMCs, including significant increases in levels of activation markers and intracellular cytokines for both innate and adaptive immune cells.

We found that PBMCs exposed to RSV-infected A549 cells had increased maturation and percentages of IFN-α-, TNF-α-, and MCP-1-producing dendritic cells and monocytes (Fig. 4 and 5). Similar to our findings, previous studies showed the ability of RSV to induce production of these cytokines in isolated human pDCs and mDCs (73, 74). However, our data show that these RSV-induced responses are impaired by the CX3C motif. The intact CX3C motif was associated with decreases in the percentages of IFN-α- and TNF-α-producing pDCs and TNF-α-producing monocytes, while the mutation of the CX3C site to CX4C and the presence of MAb 131-2G restored the production of these cytokines in innate immune cells (Fig. 5 and 6). The G protein was previously shown to affect both TLR-dependent and -independent (RIG-I/MDA5) pathways involved in the expression of IFN type I and other proinflammatory cytokines. For example, pre-

treatment of human monocytes with a G protein peptide containing the CX3C region prevented LPS-induced cytokine production (32), and both membrane and soluble forms of G protein inhibit either or both TLR3/4- and RIG-I/MDA5-mediated IFN type I induction in human monocyte-derived DCs (26). Our data suggest that the RSV G protein can affect TLR-dependent/independent signaling pathways, probably through CX3C binding to the fractalkine receptor CX3CR1. The majority of effector immune cells, including dendritic cells and monocytes, express CX3CR1 (19–21). Expression of this receptor allows them to penetrate inflamed tissues through the chemoattractive function of the CX3CR1 ligand fractalkine. A substantial role for the fractalkine-CX3CR1 interaction has been well documented for chronic inflammatory cardiovascular, neuronal, and lung diseases (75–77). CX3CR1 also appears to play an important role in pattern recognition receptor (PRR)-mediated innate immune responses. For instance, CX3CR1-deficient mice have decreased expression levels of TLR4 (78) as well as impaired bacterial clearance and production of TNF-α and IFN-γ by macrophages (79). In addition, CX3CR1 signaling has been shown to increase the activation of NF-κB (79), the common transcriptional factor in the production of antiviral and inflammatory cytokines (80).

We also found that the CX3C motif in the RSV G protein affected the adaptive immune response, as indicated by diminished percentages of IFN-γ-producing effector/memory T cells compared to the CX4C virus and treatment with $F(ab')_2$ 131-2G (Fig. 7 and 8). These data are consistent with previous studies in murine models showing a downregulation of Th1-mediated immune responses by the RSV CX3C motif (40, 41). Fraticelli et al. have shown that CX3CR1 was predominantly expressed by Th1-polarized cells and that Th1 but not Th2 cells responded to fractalkine stimulation (81). Our data suggest that the RSV G protein, which competes with fractalkine for CX3CR1 binding, may prevent this stimulation and suppress Th1-biased inflammatory responses. Interestingly, certain CX3CR1 haplotypes were found to be associated with an increased risk of severe RSV bronchiolitis in infants (82). The same single-nucleotide polymorphisms in the CX3CR1 gene were shown to confer low-affinity binding between CX3CR1 and fractalkine (83–85).

In conclusion, in this *in vitro* model of human RSV infection, we demonstrate that the RSV G protein CX3C motif has an impact on virus-host interactions in A549 human airway epithelial cells, immune cells, and their interplay and is likely an important determinant for the course of human RSV infection. The CX3C motif in the RSV G protein may be a target for future vaccine and antiviral drug development. An understanding of the mechanisms of CX3C-induced impairment of the host immune response should help clarify its role in treating and preventing RSV disease.

ACKNOWLEDGMENTS

This work was supported by NIH grant 1U19AI095227, funding from Children's Healthcare of Atlanta, support from the Immunology Core of Emory Children's Pediatric Research Center, and Emory vaccinology training grant (VTP) T32 5T32AI074492-03.

REFERENCES

1. **Shay DK, Holman RC, Newman RD, Liu LL, Stout JW, Anderson LJ.** 1999. Bronchiolitis-associated hospitalizations among US children, 1980-1996. JAMA **282:**1440–1446.
2. **Nair H, Nokes DJ, Gessner BD, Dherani M, Madhi SA, Singleton RJ, O'Brien KL, Roca A, Wright PF, Bruce N, Chandran A, Theodoratou E, Sutanto A, Sedyaningsih ER, Ngama M, Munywoki PK, Kartasasmita C, Simoes EA, Rudan I, Weber MW, Campbell H.** 2010. Global burden of acute lower respiratory infections due to respiratory syncytial virus in young children: a systematic review and meta-analysis. Lancet **375:**1545–1555.
3. **Falsey AR, Hennessey PA, Formica MA, Cox C, Walsh EE.** 2005. Respiratory syncytial virus infection in elderly and high-risk adults. N. Engl. J. Med. **352:**1749–1759.
4. **Hall CB, Weinberg GA, Iwane MK, Blumkin AK, Edwards KM, Staat MA, Auinger P, Griffin MR, Poehling KA, Erdman D, Grijalva CG, Zhu Y, Szilagyi P.** 2009. The burden of respiratory syncytial virus infection in young children. N. Engl. J. Med. **360:**588–598.
5. **Kim HW, Canchola JG, Brandt CD, Pyles G, Chanock RM, Jensen K, Parrott RH.** 1969. Respiratory syncytial virus disease in infants despite prior administration of antigenic inactivated vaccine. Am. J. Epidemiol. **89:**422–434.
6. **Fulginiti VA, Eller JJ, Sieber OF, Joyner JW, Minamitani M, Meiklejohn G.** 1969. Respiratory virus immunization. I. A field trial of two inactivated respiratory virus vaccines; an aqueous trivalent parainfluenza virus vaccine and an alum-precipitated respiratory syncytial virus vaccine. Am. J. Epidemiol. **89:**435–448.
7. **Chin J, Magoffin RL, Shearer LA, Schieble JH, Lennette EH.** 1969. Field evaluation of a respiratory syncytial virus vaccine and a trivalent parainfluenza virus vaccine in a pediatric population. Am. J. Epidemiol. **89:**449–463.
8. **Kapikian AZ, Mitchell RH, Chanock RM, Shvedoff RA, Stewart CE.** 1969. An epidemiologic study of altered clinical reactivity to respiratory syncytial (RS) virus infection in children previously vaccinated with an inactivated RS virus vaccine. Am. J. Epidemiol. **89:**405–421.
9. **Graham BS.** 2011. Biological challenges and technological opportunities for respiratory syncytial virus vaccine development. Immunol. Rev. **239:**149–166.
10. **Olmsted RA, Elango N, Prince GA, Murphy BR, Johnson PR, Moss B, Chanock RM, Collins PL.** 1986. Expression of the F glycoprotein of respiratory syncytial virus by a recombinant vaccinia virus: comparison of the individual contributions of the F and G glycoproteins to host immunity. Proc. Natl. Acad. Sci. U. S. A. **83:**7462–7466.
11. **Stott EJ, Taylor G, Ball LA, Anderson K, Young KK, King AM, Wertz GW.** 1987. Immune and histopathological responses in animals vaccinated with recombinant vaccinia viruses that express individual genes of human respiratory syncytial virus. J. Virol. **61:**3855–3861.
12. **Connors M, Collins PL, Firestone CY, Murphy BR.** 1991. Respiratory syncytial virus (RSV) F, G, M2 (22K), and N proteins each induce resistance to RSV challenge, but resistance induced by M2 and N proteins is relatively short-lived. J. Virol. **65:**1634–1637.
13. **Anderson LJ, Heilman CA.** 1995. Protective and disease-enhancing immune responses to respiratory syncytial virus. J. Infect. Dis. **171:**1–7.
14. **Melero JA, Garcia-Barreno B, Martinez I, Pringle CR, Cane PA.** 1997. Antigenic structure, evolution and immunobiology of human respiratory syncytial virus attachment (G) protein. J. Gen. Virol. **78:**2411–2418.
15. **Collins PL, Crowe JE, Jr.** 2007. Respiratory syncytial virus and metapneumovirus, p 1601–1646. *In* Knipe DM, Griffin DE, Lamb RA, Straus SE, Howley PM, Martin MA, Roizman B (ed), Fields virology, 5th ed, vol 2. Lippincott Williams & Wilkins, Philadelphia, PA.
16. **Trento A, Casas I, Calderon A, Garcia-Garcia ML, Calvo C, Perez-Brena P, Melero JA.** 2010. Ten years of global evolution of the human respiratory syncytial virus BA genotype with a 60-nucleotide duplication in the G protein gene. J. Virol. **84:**7500–7512.
17. **Tripp RA, Jones LP, Haynes LM, Zheng H, Murphy PM, Anderson LJ.** 2001. CX3C chemokine mimicry by respiratory syncytial virus G glycoprotein. Nat. Immunol. **2:**732–738.
18. **Harrison JK, Jiang Y, Chen S, Xia Y, Maciejewski D, McNamara RK, Streit WJ, Salafranca MN, Adhikari S, Thompson DA, Botti P, Bacon KB, Feng L.** 1998. Role for neuronally derived fractalkine in mediating interactions between neurons and CX3CR1-expressing microglia. Proc. Natl. Acad. Sci. U. S. A. **95:**10896–10901.
19. **Imai T, Hieshima K, Haskell C, Baba M, Nagira M, Nishimura M, Kakizaki M, Takagi S, Nomiyama H, Schall TJ, Yoshie O.** 1997. Identification and molecular characterization of fractalkine receptor CX3CR1, which mediates both leukocyte migration and adhesion. Cell **91:**521–530.
20. **Bar-On L, Birnberg T, Lewis KL, Edelson BT, Bruder D, Hildner K, Buer J, Murphy KM, Reizis B, Jung S.** 2010. CX3CR1+ CD8alpha+

dendritic cells are a steady-state population related to plasmacytoid dendritic cells. Proc. Natl. Acad. Sci. U. S. A. **107:**14745–14750.
21. **Nishimura M, Umehara H, Nakayama T, Yoneda O, Hieshima K, Kakizaki M, Dohmae N, Yoshie O, Imai T.** 2002. Dual functions of fractalkine/CX3C ligand 1 in trafficking of perforin+/granzyme B+ cytotoxic effector lymphocytes that are defined by CX3CR1 expression. J. Immunol. **168:**6173–6180.
22. **Fong AM, Robinson LA, Steeber DA, Tedder TF, Yoshie O, Imai T, Patel DD.** 1998. Fractalkine and CX3CR1 mediate a novel mechanism of leukocyte capture, firm adhesion, and activation under physiologic flow. J. Exp. Med. **188:**1413–1419.
23. **Bembridge GP, Garcia-Beato R, Lopez JA, Melero JA, Taylor G.** 1998. Subcellular site of expression and route of vaccination influence pulmonary eosinophilia following respiratory syncytial virus challenge in BALB/c mice sensitized to the attachment G protein. J. Immunol. **161:**2473–2480.
24. **Hancock GE, Speelman DJ, Heers K, Bortell E, Smith J, Cosco C.** 1996. Generation of atypical pulmonary inflammatory responses in BALB/c mice after immunization with the native attachment (G) glycoprotein of respiratory syncytial virus. J. Virol. **70:**7783–7791.
25. **Johnson TR, Graham BS.** 1999. Secreted respiratory syncytial virus G glycoprotein induces interleukin-5 (IL-5), IL-13, and eosinophilia by an IL-4-independent mechanism. J. Virol. **73:**8485–8495.
26. **Shingai M, Azuma M, Ebihara T, Sasai M, Funami K, Ayata M, Ogura H, Tsutsumi H, Matsumoto M, Seya T.** 2008. Soluble G protein of respiratory syncytial virus inhibits Toll-like receptor 3/4-mediated IFN-beta induction. Int. Immunol. **20:**1169–1180.
27. **Sparer TE, Matthews S, Hussell T, Rae AJ, Garcia-Barreno B, Melero JA, Openshaw PJ.** 1998. Eliminating a region of respiratory syncytial virus attachment protein allows induction of protective immunity without vaccine-enhanced lung eosinophilia. J. Exp. Med. **187:**1921–1926.
28. **Tebbey PW, Hagen M, Hancock GE.** 1998. Atypical pulmonary eosinophilia is mediated by a specific amino acid sequence of the attachment (G) protein of respiratory syncytial virus. J. Exp. Med. **188:**1967–1972.
29. **Arnold R, Konig B, Werchau H, Konig W.** 2004. Respiratory syncytial virus deficient in soluble G protein induced an increased proinflammatory response in human lung epithelial cells. Virology **330:**384–397.
30. **Ray R, Hoft DF, Meyer K, Brown R, Lagging LM, Belshe RB.** 2001. Immunoregulatory role of secreted glycoprotein G from respiratory syncytial virus. Virus Res. **75:**147–154.
31. **Johnson TR, McLellan JS, Graham BS.** 2012. Respiratory syncytial virus glycoprotein G interacts with DC-SIGN and L-SIGN to activate ERK1 and ERK2. J. Virol. **86:**1339–1347.
32. **Polack FP, Irusta PM, Hoffman SJ, Schiatti MP, Melendi GA, Delgado MF, Laham FR, Thumar B, Hendry RM, Melero JA, Karron RA, Collins PL, Kleeberger SR.** 2005. The cysteine-rich region of respiratory syncytial virus attachment protein inhibits innate immunity elicited by the virus and endotoxin. Proc. Natl. Acad. Sci. U. S. A. **102:**8996–9001.
33. **Bukreyev A, Serra ME, Laham FR, Melendi GA, Kleeberger SR, Collins PL, Polack FP.** 2006. The cysteine-rich region and secreted form of the attachment G glycoprotein of respiratory syncytial virus enhance the cytotoxic T-lymphocyte response despite lacking major histocompatibility complex class I-restricted epitopes. J. Virol. **80:**5854–5861.
34. **Melendi GA, Bridget D, Monsalvo AC, Laham FF, Acosta P, Delgado MF, Polack FP, Irusta PM.** 2011. Conserved cysteine residues within the attachment G glycoprotein of respiratory syncytial virus play a critical role in the enhancement of cytotoxic T-lymphocyte responses. Virus Genes **42:**46–54.
35. **Oshansky CM, Krunkosky TM, Barber J, Jones LP, Tripp RA.** 2009. Respiratory syncytial virus proteins modulate suppressors of cytokine signaling 1 and 3 and the type I interferon response to infection by a Toll-like receptor pathway. Viral Immunol. **22:**147–161.
36. **Tripp RA, Dakhama A, Jones LP, Barskey A, Gelfand EW, Anderson LJ.** 2003. The G glycoprotein of respiratory syncytial virus depresses respiratory rates through the CX3C motif and substance P. J. Virol. **77:**6580–6584.
37. **Tripp RA, Jones L, Anderson LJ.** 2000. Respiratory syncytial virus G and/or SH glycoproteins modify CC and CXC chemokine mRNA expression in the BALB/c mouse. J. Virol. **74:**6227–6229.
38. **Bukreyev A, Yang L, Fricke J, Cheng L, Ward JM, Murphy BR, Collins PL.** 2008. The secreted form of respiratory syncytial virus G glycoprotein helps the virus evade antibody-mediated restriction of replication by acting as an antigen decoy and through effects on Fc receptor-bearing leukocytes. J. Virol. **82:**12191–12204.
39. **Bukreyev A, Yang L, Collins PL.** 2012. The secreted G protein of human respiratory syncytial virus antagonizes antibody-mediated restriction of replication involving macrophages and complement. J. Virol. **86:**10880–10884.
40. **Harcourt J, Alvarez R, Jones LP, Henderson C, Anderson LJ, Tripp RA.** 2006. Respiratory syncytial virus G protein and G protein CX3C motif adversely affect CX3CR1+ T cell responses. J. Immunol. **176:**1600–1608.
41. **Haynes LM, Jones LP, Barskey A, Anderson LJ, Tripp RA.** 2003. Enhanced disease and pulmonary eosinophilia associated with formalin-inactivated respiratory syncytial virus vaccination are linked to G glycoprotein CX3C-CX3CR1 interaction and expression of substance P. J. Virol. **77:**9831–9844.
42. **Oshansky CM, Barber JP, Crabtree J, Tripp RA.** 2010. Respiratory syncytial virus F and G proteins induce interleukin 1alpha, CC, and CXC chemokine responses by normal human bronchoepithelial cells. J. Infect. Dis. **201:**1201–1207.
43. **Konig B, Streckert HJ, Krusat T, Konig W.** 1996. Respiratory syncytial virus G-protein modulates cytokine release from human peripheral blood mononuclear cells. J. Leukoc. Biol. **59:**403–406.
44. **Qin L, Hu CP, Feng JT, Xia Q.** 2011. Activation of lymphocytes induced by bronchial epithelial cells with prolonged RSV infection. PLoS One **6:**e27113. doi:10.1371/journal.pone.0027113.
45. **Giard DJ, Aaronson SA, Todaro GJ, Arnstein P, Kersey JH, Dosik H, Parks WP.** 1973. In vitro cultivation of human tumors: establishment of cell lines derived from a series of solid tumors. J. Natl. Cancer Inst. **51:**1417–1423.
46. **Mitra R, Baviskar P, Duncan-Decocq RR, Patel D, Oomens AG.** 2012. The human respiratory syncytial virus matrix protein is required for maturation of viral filaments. J. Virol. **86:**4432–4443.
47. **Anderson LJ, Hierholzer JC, Stone YO, Tsou C, Fernie BF.** 1986. Identification of epitopes on respiratory syncytial virus proteins by competitive binding immunoassay. J. Clin. Microbiol. **23:**475–480.
48. **Anderson LJ, Hierholzer JC, Bingham PG, Stone YO.** 1985. Microneutralization test for respiratory syncytial virus based on an enzyme immunoassay. J. Clin. Microbiol. **22:**1050–1052.
49. **Kodani M, Yang G, Conklin LM, Travis TC, Whitney CG, Anderson LJ, Schrag SJ, Taylor TH, Jr, Beall BW, Breiman RF, Feikin DR, Njenga MK, Mayer LW, Oberste MS, Tondella ML, Winchell JM, Lindstrom SL, Erdman DD, Fields BS.** 2011. Application of TaqMan low-density arrays for simultaneous detection of multiple respiratory pathogens. J. Clin. Microbiol. **49:**2175–2182.
50. **Prussin C, Metcalfe DD.** 1995. Detection of intracytoplasmic cytokine using flow cytometry and directly conjugated anti-cytokine antibodies. J. Immunol. Methods **188:**117–128.
51. **Ank N, West H, Bartholdy C, Eriksson K, Thomsen AR, Paludan SR.** 2006. Lambda interferon (IFN-lambda), a type III IFN, is induced by viruses and IFNs and displays potent antiviral activity against select virus infections in vivo. J. Virol. **80:**4501–4509.
52. **Kotenko SV, Gallagher G, Baurin VV, Lewis-Antes A, Shen M, Shah NK, Langer JA, Sheikh F, Dickensheets H, Donnelly RP.** 2003. IFN-lambdas mediate antiviral protection through a distinct class II cytokine receptor complex. Nat. Immunol. **4:**69–77.
53. **Zhou Z, Hamming OJ, Ank N, Paludan SR, Nielsen AL, Hartmann R.** 2007. Type III interferon (IFN) induces a type I IFN-like response in a restricted subset of cells through signaling pathways involving both the Jak-STAT pathway and the mitogen-activated protein kinases. J. Virol. **81:**7749–7758.
54. **Freeman GJ, Gribben JG, Boussiotis VA, Ng JW, Restivo VA, Jr, Lombard LA, Gray GS, Nadler LM.** 1993. Cloning of B7-2: a CTLA-4 counter-receptor that costimulates human T cell proliferation. Science **262:**909–911.
55. **Munro JM, Freedman AS, Aster JC, Gribben JG, Lee NC, Rhynhart KK, Banchereau J, Nadler LM.** 1994. In vivo expression of the B7 costimulatory molecule by subsets of antigen-presenting cells and the malignant cells of Hodgkin's disease. Blood **83:**793–798.
56. **Piccioli D, Tavarini S, Borgogni E, Steri V, Nuti S, Sammicheli C, Bardelli M, Montagna D, Locatelli F, Wack A.** 2007. Functional specialization of human circulating CD16 and CD1c myeloid dendritic-cell subsets. Blood **109:**5371–5379.
57. **Hart DN.** 1997. Dendritic cells: unique leukocyte populations which control the primary immune response. Blood **90:**3245–3287.

58. **Kawai T, Akira S.** 2006. Innate immune recognition of viral infection. Nat. Immunol. **7:**131–137.
59. **Sallusto F, Lenig D, Forster R, Lipp M, Lanzavecchia A.** 1999. Two subsets of memory T lymphocytes with distinct homing potentials and effector functions. Nature **401:**708–712.
60. **Koch S, Larbi A, Derhovanessian E, Ozcelik D, Naumova E, Pawelec G.** 2008. Multiparameter flow cytometric analysis of CD4 and CD8 T cell subsets in young and old people. Immun. Ageing **5:**6. doi:10.1186/1742-4933-5-6.
61. **Kauvar LM, Harcourt JL, Haynes LM, Tripp RA.** 2010. Therapeutic targeting of respiratory syncytial virus G-protein. Immunotherapy **2:**655–661.
62. **Sheppard P, Kindsvogel W, Xu W, Henderson K, Schlutsmeyer S, Whitmore TE, Kuestner R, Garrigues U, Birks C, Roraback J, Ostrander C, Dong D, Shin J, Presnell S, Fox B, Haldeman B, Cooper E, Taft D, Gilbert T, Grant FJ, Tackett M, Krivan W, McKnight G, Clegg C, Foster D, Klucher KM.** 2003. IL-28, IL-29 and their class II cytokine receptor IL-28R. Nat. Immunol. **4:**63–68.
63. **Ank N, Iversen MB, Bartholdy C, Staeheli P, Hartmann R, Jensen UB, Dagnaes-Hansen F, Thomsen AR, Chen Z, Haugen H, Klucher K, Paludan SR.** 2008. An important role for type III interferon (IFN-lambda/IL-28) in TLR-induced antiviral activity. J. Immunol. **180:**2474–2485.
64. **Mordstein M, Kochs G, Dumoutier L, Renauld JC, Paludan SR, Klucher K, Staeheli P.** 2008. Interferon-lambda contributes to innate immunity of mice against influenza A virus but not against hepatotropic viruses. PLoS Pathog. **4:**e1000151. doi:10.1371/journal.ppat.1000151.
65. **Sommereyns C, Paul S, Staeheli P, Michiels T.** 2008. IFN-lambda (IFN-lambda) is expressed in a tissue-dependent fashion and primarily acts on epithelial cells in vivo. PLoS Pathog. **4:**e1000017. doi:10.1371/journal.ppat.1000017.
66. **Okabayashi T, Kojima T, Masaki T, Yokota S, Imaizumi T, Tsutsumi H, Himi T, Fujii N, Sawada N.** 2011. Type-III interferon, not type-I, is the predominant interferon induced by respiratory viruses in nasal epithelial cells. Virus Res. **160:**360–366.
67. **Villenave R, Thavagnanam S, Sarlang S, Parker J, Douglas I, Skibinski G, Heaney LG, McKaigue JP, Coyle PV, Shields MD, Power UF.** 2012. In vitro modeling of respiratory syncytial virus infection of pediatric bronchial epithelium, the primary target of infection in vivo. Proc. Natl. Acad. Sci. U. S. A. **109:**5040–5045.
68. **Ioannidis I, McNally B, Willette M, Peeples ME, Chaussabel D, Durbin JE, Ramilo O, Mejias A, Flano E.** 2012. Plasticity and virus specificity of the airway epithelial cell immune response during respiratory virus infection. J. Virol. **86:**5422–5436.
69. **Lo MS, Brazas RM, Holtzman MJ.** 2005. Respiratory syncytial virus nonstructural proteins NS1 and NS2 mediate inhibition of Stat2 expression and alpha/beta interferon responsiveness. J. Virol. **79:**9315–9319.
70. **Bossert B, Marozin S, Conzelmann KK.** 2003. Nonstructural proteins NS1 and NS2 of bovine respiratory syncytial virus block activation of interferon regulatory factor 3. J. Virol. **77:**8661–8668.
71. **Spann KM, Tran KC, Collins PL.** 2005. Effects of nonstructural proteins NS1 and NS2 of human respiratory syncytial virus on interferon regulatory factor 3, NF-kappaB, and proinflammatory cytokines. J. Virol. **79:**5353–5362.
72. **Moore EC, Barber J, Tripp RA.** 2008. Respiratory syncytial virus (RSV) attachment and nonstructural proteins modify the type I interferon response associated with suppressor of cytokine signaling (SOCS) proteins and IFN-stimulated gene-15 (ISG15). Virol. J. **5:**116. doi:10.1186/1743-422X-5-116.
73. **Johnson TR, Johnson CN, Corbett KS, Edwards GC, Graham BS.** 2011. Primary human mDC1, mDC2, and pDC dendritic cells are differentially infected and activated by respiratory syncytial virus. PLoS One **6:**e16458. doi:10.1371/journal.pone.0016458.
74. **Guerrero-Plata A, Casola A, Suarez G, Yu X, Spetch L, Peeples ME, Garofalo RP.** 2006. Differential response of dendritic cells to human metapneumovirus and respiratory syncytial virus. Am. J. Respir. Cell Mol. Biol. **34:**320–329.
75. **Denes A, Ferenczi S, Halasz J, Kornyei Z, Kovacs KJ.** 2008. Role of CX3CR1 (fractalkine receptor) in brain damage and inflammation induced by focal cerebral ischemia in mouse. J. Cereb. Blood Flow Metab. **28:**1707–1721.
76. **Liu H, Jiang D.** 2011. Fractalkine/CX3CR1 and atherosclerosis. Clin. Chim. Acta **412:**1180–1186.
77. **Zhang J, Patel JM.** 2010. Role of the CX3CL1-CX3CR1 axis in chronic inflammatory lung diseases. Int. J. Clin. Exp. Med. **3:**233–244.
78. **Ross RJ, Zhou M, Shen D, Fariss RN, Ding X, Bojanowski CM, Tuo J, Chan CC.** 2008. Immunological protein expression profile in Ccl2/Cx3cr1 deficient mice with lesions similar to age-related macular degeneration. Exp. Eye Res. **86:**675–683.
79. **Ishida Y, Hayashi T, Goto T, Kimura A, Akimoto S, Mukaida N, Kondo T.** 2008. Essential involvement of CX3CR1-mediated signals in the bactericidal host defense during septic peritonitis. J. Immunol. **181:**4208–4218.
80. **Tak PP, Firestein GS.** 2001. NF-kappaB: a key role in inflammatory diseases. J. Clin. Invest. **107:**7–11.
81. **Fraticelli P, Sironi M, Bianchi G, D'Ambrosio D, Albanesi C, Stoppacciaro A, Chieppa M, Allavena P, Ruco L, Girolomoni G, Sinigaglia F, Vecchi A, Mantovani A.** 2001. Fractalkine (CX3CL1) as an amplification circuit of polarized Th1 responses. J. Clin. Invest. **107:**1173–1181.
82. **Amanatidou V, Sourvinos G, Apostolakis S, Tsilimigaki A, Spandidos DA.** 2006. T280M variation of the CX3C receptor gene is associated with increased risk for severe respiratory syncytial virus bronchiolitis. Pediatr. Infect. Dis. J. **25:**410–414.
83. **McDermott DH, Fong AM, Yang Q, Sechler JM, Cupples LA, Merrell MN, Wilson PW, D'Agostino RB, O'Donnell CJ, Patel DD, Murphy PM.** 2003. Chemokine receptor mutant CX3CR1-M280 has impaired adhesive function and correlates with protection from cardiovascular disease in humans. J. Clin. Invest. **111:**1241–1250.
84. **Lavergne E, Labreuche J, Daoudi M, Debre P, Cambien F, Deterre P, Amarenco P, Combadiere C.** 2005. Adverse associations between CX3CR1 polymorphisms and risk of cardiovascular or cerebrovascular disease. Arterioscler. Thromb. Vasc. Biol. **25:**847–853.
85. **Moatti D, Faure S, Fumeron F, Amara Mel W, Seknadji P, McDermott DH, Debre P, Aumont MC, Murphy PM, de Prost D, Combadiere C.** 2001. Polymorphism in the fractalkine receptor CX3CR1 as a genetic risk factor for coronary artery disease. Blood **97:**1925–1928.